Antiviral Research 100 (2013) 215–219

Contents lists available at ScienceDirect

Antiviral Research

journal homepage: www.elsevier.com/locate/antiviral

Short Communication

Arbidol inhibits viral entry by interfering with clathrin-dependent trafficking

Julie Blaising [a,1,2], Pierre L. Lévy [b,1], Stephen J. Polyak [c], Megan Stanifer [d], Steeve Boulant [d,*,1], Eve-Isabelle Pécheur [a,*,1,2]

[a] IBCP, UMR 5086, CNRS, University of Lyon, Lyon, France
[b] CRCL, Inserm U1052, CNRS 5286, University of Lyon, Lyon, France
[c] Dept of Laboratory Medicine and Global Health, University of Washington, Seattle, WA, USA
[d] Dept of Infectious Diseases, Virology, CHS Nachwuchsgruppe am CellNetworks Cluster und DKFZ, University of Heidelberg, Germany

ARTICLE INFO

Article history:
Received 24 May 2013
Revised 12 July 2013
Accepted 8 August 2013
Available online 25 August 2013

Keywords:
Hepatitis C virus
Vesicular stomatitis virus
Reovirus
Arbidol
Broad spectrum antiviral
Entry

ABSTRACT

Arbidol (ARB) is a broad-spectrum antiviral displaying activity against a number of enveloped and non-enveloped viruses. It was described as a viral entry inhibitor and shown to interact at the molecular level with lipid membranes and viral fusion glycoproteins to impede viral entry and fusion. However its mechanism of action at the cellular level remains unknown. Here, by using live-cell confocal imaging and the hepatitis C virus as a model virus, we show that ARB affects clathrin-mediated endocytosis by impeding dynamin-2-induced membrane scission. Moreover it induces the intracellular accumulation of clathrin-coated structures where viral particles are trapped. Collectively, our results shed light on the mechanistic aspects of ARB antiviral activity and suggest that ARB could prevent cell infection by viruses that enter through clathrin-mediated endocytosis.

Antiviral drug development has led to significant advances in the control of globally prevalent viral infections including hepatitis C virus (HCV) and human immunodeficiency virus (HIV). Nonetheless, there are current gaps in the armamentarium against (re-)emerging viruses causing problems for global control and eradication, especially in cases of major outbreaks. Arbidol (ARB), a drug already licensed in Russia and China against flu, was described as a broad-spectrum antiviral able to prevent infection of enveloped and non-enveloped viruses (Boriskin et al., 2008; Brooks et al., 2004, 2012; Delogu et al., 2011). It was shown to inhibit viral replication (Boriskin et al., 2006; Brooks et al., 2012; Chai et al., 2006; Delogu et al., 2011) and entry (reviewed in Boriskin et al., 2008; Leneva et al., 2009; Teissier et al., 2010). Cell entry of viruses is an attractive target to therapeutic intervention, with opportunities to protect 'naive' cells. At the atomic and molecular levels, ARB was shown to display a dual binding capacity: on lipid membrane interfaces (Pécheur et al., 2007; Teissier et al., 2011; Villalain, 2010) and on specific residues within the viral fusion glycoprotein(s) (Leneva et al., 2009; Teissier et al., 2011), thereby altering membrane fluidity, hindering conformational rearrangements in viral glycoproteins and blocking viral fusion. In spite of these documented studies, the mechanism by which ARB blocks viral entry at the cellular level remains unknown. Here we investigated this feature by using live-cell confocal imaging and HCV as a model of enveloped virus.

We first studied the effect of ARB on HCV intracellular trafficking in Huh7.5 hepatoma cells. Cells were pretreated or not with 11 μM ARB and synchronized on ice for 1 h with HCV grown in cell culture (HCVcc, MOI 1). This concentration was chosen since it did not cause any cytotoxicity, constituted the IC_{50} of HCV infectivity and induced maximal inhibition of HCV fusion *in vitro* (Blaising et al., 2013; Boriskin et al., 2006; Haid et al., 2009; Pécheur et al., 2007). After washing unbound virus, cells were transferred to

Abbreviations: ARB, arbidol; CCP, clathrin-coated pit; CCV, clathrin-coated vesicle; CME, clathrin-mediated endocytosis; Clc, clathrin light chain; HCV, hepatitis C virus; HCVcc, HCV grown in cell culture; HCVpp, HCV pseudotyped particles; ISVP, infectious subvirion particle; MOI, multiplicity of infection; Trf, transferrin; VSV, vesicular stomatitis virus.

* Corresponding authors. Address: CHS Nachwuchsgruppe am CellNetworks Cluster und DKFZ, Department of Infectious Diseases, Virology, Im Neuenheimer Feld 581, University Heidelberg, Germany. Tel.: +49 6221 42 1560 (S. Boulant), CRCL, Inserm U1052, CNRS 5286, University of Lyon, 69424 Lyon cedex 03, France. Tel.: +33 4 7268 1975 (E.-I. Pécheur).

E-mail addresses: s.boulant@dkfz-heidelberg.de (S. Boulant), eve-isabelle.pecheur@inserm.fr (E.-I. Pécheur).

[1] These authors contributed equally to this work.

[2] Present address: CRCL, Inserm U1052, CNRS 5286, University of Lyon, Lyon, France.

0166-3542/$ - see front matter © 2013 Elsevier B.V. All rights reserved.
http://dx.doi.org/10.1016/j.antiviral.2013.08.008

37 °C to initiate viral entry, then fixed at early (15 min) and late (60 min) stages of infection, and co-immunostained for HCV core and markers of early or late endocytic compartments (clathrin or Lamp1 respectively), as described (Blaising et al., 2013). In the absence of ARB, HCV mainly colocalized with clathrin-positive structures 15 min post-infection; after 60 min, particles no longer colocalized with clathrin but coincided with Lamp1 (Fig. 1A; quantification in B), indicating that the virus had moved from endocytic vesicles to late endosomes. Strikingly, in ARB-treated cells, virions were confined in clathrin-positive structures at early and late times post-infection (Fig. 1), suggesting that ARB impedes HCV intracellular trafficking from early to late endosomal compartments.

We then followed clathrin-mediated endocytosis (CME) into living cells by time-lapse confocal microscopy, using HCV-pseudotyped retroviral particles (HCVpp, Bartosch et al., 2003; Blaising et al., 2013). Concentrated HCVpp were labeled with the lipophilic rhodamine dye R_{18}, thoroughly purified and characterized as described in (Blaising et al., 2013). Huh7.5 cells expressing a clathrin-GFP fusion protein, pretreated or not with ARB, were infected with R_{18}-HCVpp. After temperature shift, particle internalization was followed by imaging five times per second for several minutes (Movie S1). A typical HCV entry event is shown Fig. 2A (top): after binding, HCV associated with a discrete clathrin-GFP spot (30s). The clathrin-GFP signal around the virion then increased (60s), followed by a rapid disappearance of the clathrin signal (88s), suggesting the internalization of the virus via clathrin-coated pits (CCPs), followed by rapid uncoating of clathrin-coated vesicles (CCVs). In ARB-treated cells, HCV remained confined in CCVs for a greater period of time (305s). Tracking analyses revealed an overall impediment to HCV movement and speed in ARB- *vs* mock-treated cells (Fig. 2A bottom; 2B; Movie S2).

Quantification of the number of internalized R_{18}-HCVpp normalized to the cell area was performed as a function of time. In untreated cells, the number of HCV particles in cells increased over the first 15 min, corresponding to the virion internalization phase (Mock, Fig. 2C). It then decreased over the next 50 min, corresponding to HCVpp fusion with endosome membranes, associated with disappearance of the fluorescence signal from viral particles or degradation of HCVpp. In the presence of ARB, the number of cell-associated virions was significantly lower than in mock-treated cells over the first 15 min (ARB, Fig. 2C; see Fig. 4D). This number drastically increased to reach a plateau at 45 min, and was stable even when longer kinetics were followed (not shown). This suggests the absence of fusion events and/or the confinement of HCV inside stabilized clathrin-coated structures in ARB-treated cells. We next quantified the colocalization events over time of clathrin-coated structures with HCV (Fig. 2D). In mock-treated cells, the number of colocalization events was constant within the first 20 min. This corresponds to the clathrin-dependent uptake phase of HCV by cells. This number decreased at later times, when viruses have already entered cells. Upon ARB treatment, fewer virions were found associated with clathrin and this number did not significantly increase over time. This agrees with our data shown in Fig. 2A and suggests that ARB hinders HCV internalization via CCVs into hepatoma cells, leading to virion confinement in CCVs.

To test whether ARB could slow down CME as a general mechanism, we addressed both the impact of ARB on viruses known to infect cells in a clathrin-dependent manner and on the cellular uptake of clathrin-specific cargo. For this purpose we used BSC-1 cells, a canonical model system to study CME (Ehrlich et al., 2004; Blaising et al., 2013; Boulant et al., 2011). As observed with Huh7.5 cells, ARB displayed cytotoxicity only at high doses (Fig. S1). We first assessed ARB antiviral activity against vesicular stomatitis virus (VSV) and reovirus, which enter cells by CME (Cureton et al., 2009; Schulz et al., 2012). Pretreating BSC-1 cells with ARB prevented VSV infection in a dose-dependent manner, and

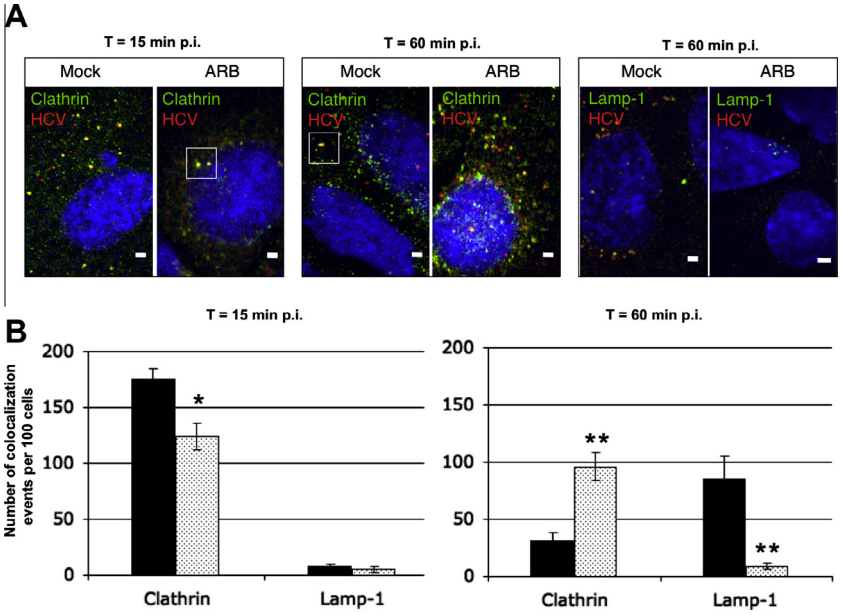

Fig. 1. ARB impedes HCV intracellular trafficking. (A) Huh7.5 cells were mock- or pre-treated with 11 μM ARB (99% pure, dissolved in ethanol/H_2O 10:90 v:v) for 30 min at 37 °C, and incubated with HCVcc clone JFH-1 (prepared and titrated as in (Wakita et al., 2005); 9.9 × 10e5 ffu/ml; MOI 1) for 1 h at 4 °C, in medium containing ARB or not. Unbound virus was washed off with cold PBS, culture medium with or without ARB was added and cells were shifted to 37 °C to initiate viral cell entry. Coverslips were fixed with 2% PFA at early (15 min) and late (60 min) stages of infection, co-immunostained for HCV core (red) and clathrin light chain or Lamp-1 (endo-lysosomal marker) (green) and imaged using a Leica Confocal Spectral TCS SP5 AOBS. Bar, 2 μm. (B) Quantification of the number of colocalization events between HCVcc and indicated endosomal marker, counted in 100 cells, mock- or ARB-treated; 15 min/60 min, time after transfer of HCV-infected cells to 37 °C. Results are mean ± SD from three independent experiments. Black bars, mock; shaded bars, ARB-treated cells. *, $p < 0.01$; **, $p < 0.005$ (unpaired *t* Student's test). (For interpretation of the references to colour in this figure legend, the reader is referred to the web version of this article.)

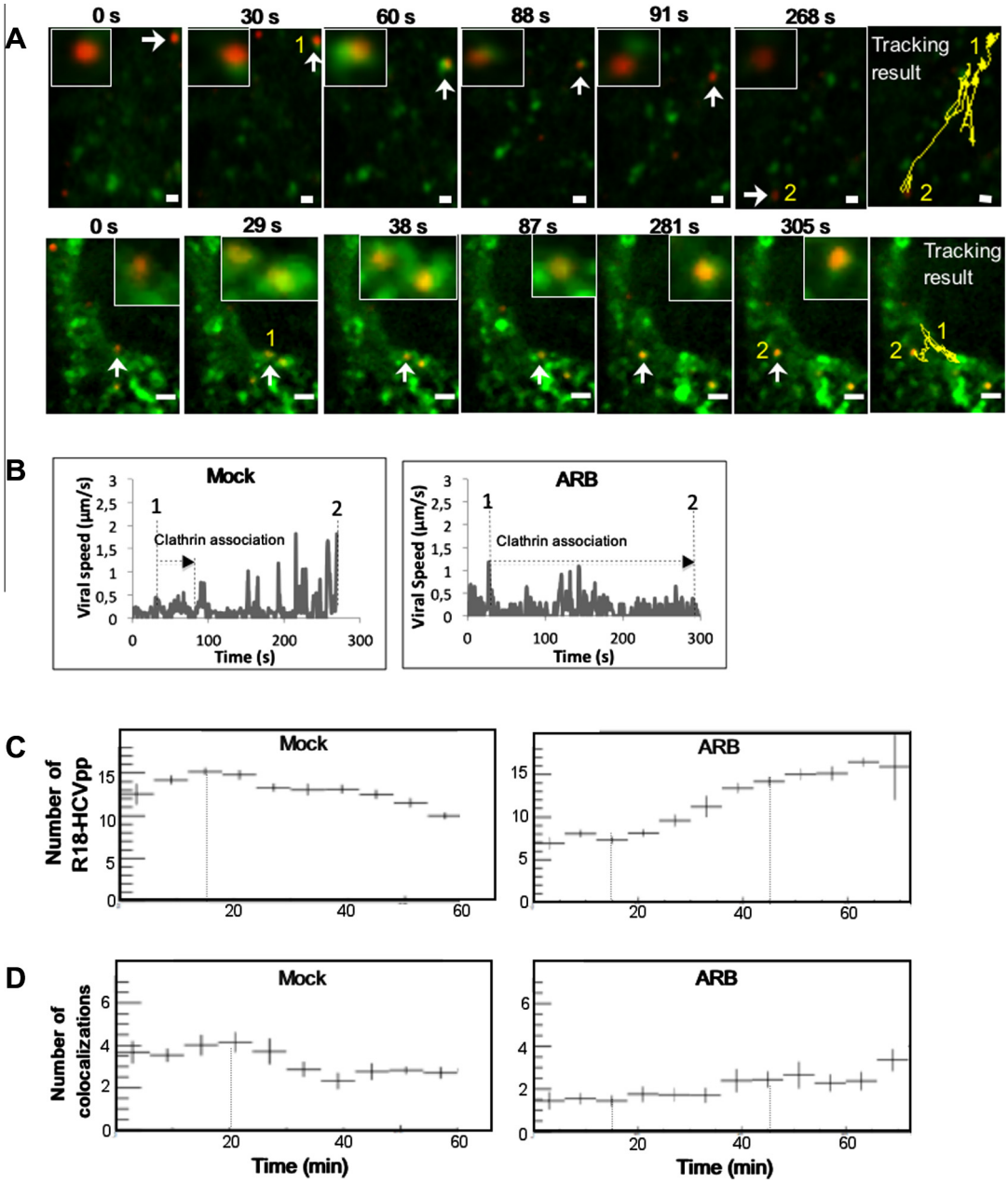

Fig. 2. ARB hinders HCV internalization. (A) Snapshots of R_{18}-labeled HCVpp (red), internalized in GFP-clathrin-coated pits (green) in mock-treated cells (Mock; Movie S1) or treated with 11 µM ARB (ARB; Movie S2). HCVpp trajectories were reconstituted using ImageJ plug-in Manual_Tracking (http://rsbweb.nih.gov/ij/plugins/track/track.html). Yellow trackings indicate beginning (1) and end (2) of HCVpp trajectory. Bar, 2 µm. (B) Viral speed recorded from similar analyses of trajectories as in A, in the absence (Mock) or presence of ARB; CME, clathrin-mediated endocytosis. (C) Number of R_{18}-HCVpp normalized to a cell area of 2000 µm^2, as a function of time in mock- or ARB-treated cells. To estimate the measurement error on the number of HCV particles, the mean value and standard deviation of these quantities were calculated using counts over a 6 min-period. Each symbol corresponds to counts performed on six individual cells. The ROOT TEfficiency method based on the Clopper–Pearson confidence limits was used (http://root.cern.ch/root/html/TEfficiency.html), since the number of events evaluated was not following a gaussian distribution. (D) Number of colocalization events between clathrin-coated structures and HCV normalized to a cell area of 2000 µm^2, as a function of time in mock- or ARB-treated cells, performed similarly as in C. (For interpretation of the references to colour in this figure legend, the reader is referred to the web version of this article.)

IC_{50s} of ARB for VSV and HCV were similar (Fig. S2A) [14 and 11 µM, respectively], strongly suggestive of a similar inhibitory mechanism of HCV and VSV infection. ARB reduced by 80% the number of reovirus-infected cells (Fig. S2B), but did not alter infection by infectious subvirion particles (ISVPs), which enter cells independently of CME (Maginnis et al., 2008; Martinez et al., 1996).

We next monitored the uptake of transferrin (Trf), a prototype cargo for CCV. In mock-treated BSC-1 cells, Trf was detected within endosomal compartments in the perinuclear region (Fig. 3A). In ARB-treated cells, very little Trf was detected intracellularly, except few Trf-loaded endosomes (Fig. 3B). Similar results were obtained using Huh7.5 cells (Fig. S3). This suggests that ARB affects CME, in line with ARB impediment on HCV particle uptake.

To gain further details on the mechanisms of ARB, we monitored the impact of ARB treatment on the dynamics of CCP formation using BSC-1 cells expressing adaptor protein-2 (AP2) fused to GFP, as described (Blaising et al., 2013; Boulant et al., 2011). Cells were mock- or ARB-treated, observed by live-cell confocal microscopy and CCP formation lifetime was determined as in (Boulant

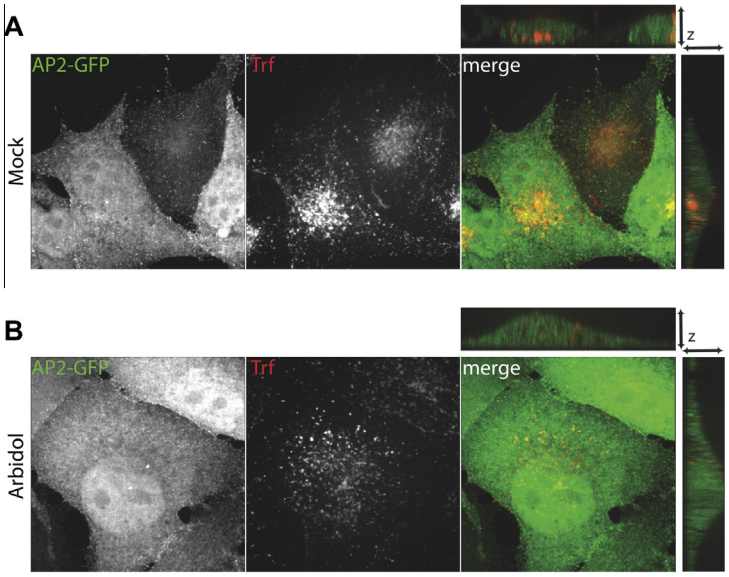

Fig. 3. ARB impairs clathrin-dependent endocytosis in BSC-1 cells. African green monkey kidney BSC-1 cells expressing AP2 σ^2 subunit fused to eGFP were plated 16 h at 37 °C prior to experiment. Cells were either mock- (A) or ARB-pretreated (B) at a final concentration of 11 μM in complete DMEM medium for 15 min. Cells were washed twice with PBS and human Trf (50 μg/ml) was added to the cells in serum-free medium, in the presence or absence (mock) of 11 μM ARB at 37 °C. After a 7 min-uptake, cells were fixed with 4% PFA, mounted on slide with prolonged gold and observed by fluorescence confocal microscopy. (For interpretation of the references to colour in this figure legend, the reader is referred to the web version of this article.)

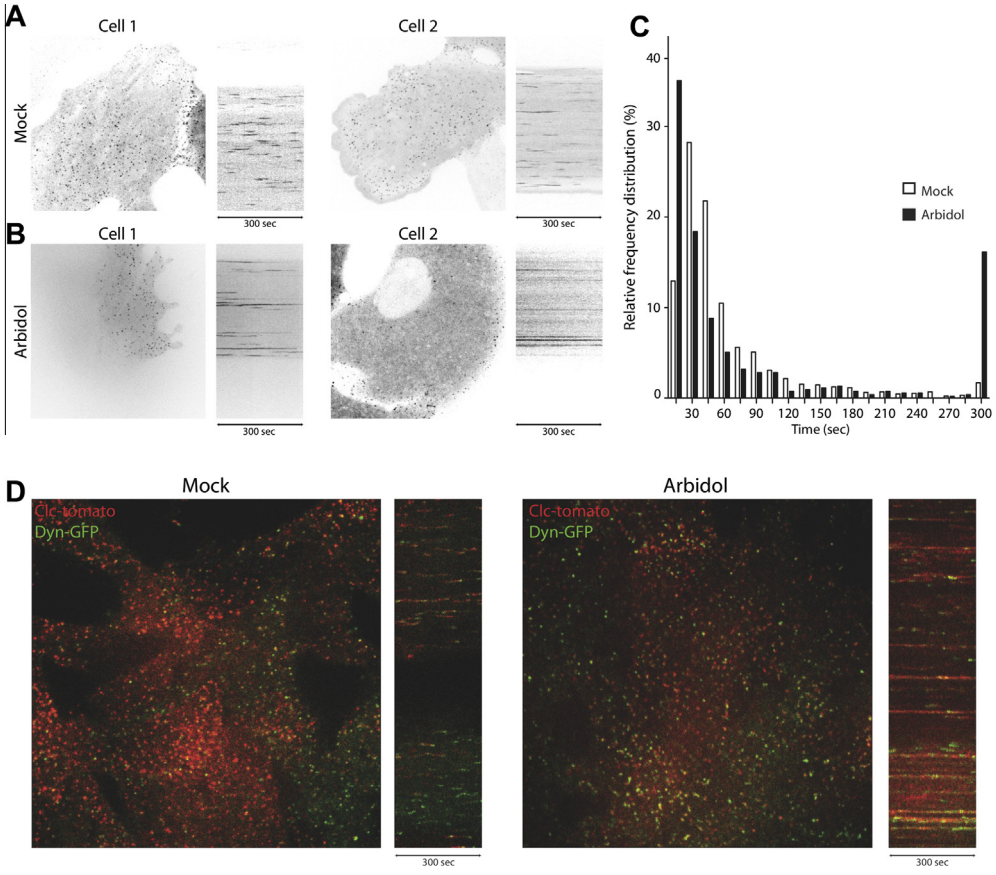

Fig. 4. ARB prevents pinching of CCPs from the plasma membrane. BSC-1 cells expressing AP2 (subunit σ′2)-GFP were seeded 16 h prior to experiments in Labteck® live cell chambers. Cells were washed once with PBS and medium was replaced by imaging medium (DMEM 2% FCS, phenol red-free) containing (B) or not (mock) 11 μM ARB (A). Dynamics of coated pit formation was monitored by live-cell spinning disk confocal microscopy, imaging every 3 s for a total time of 300 s. Clathrin-coated structures were identified using a Mat-lab IMAB software (Boulant et al., 2011) and CCPs lifetimes were determined. C. The lifetime distribution of CCPs in mock-treated cells (from A; Movies S3–5) and ARB-treated cells (from B; Movies S6–8) was plotted using a bin of 15 s. D. BSC-1 cells expressing Clc-tomato and Dyn-GFP were seeded 16 h prior to experiments. Cells were processed and imaged as described above. (For interpretation of the references to colour in this figure legend, the reader is referred to the web version of this article.)

et al., 2011). In mock-treated cells, most pits were dynamic (appearing/disappearing) during the 300s-imaging period, as seen on kymographs (time projections, Fig. 4A), CCP lifetime distribution (Fig. 4C) and in movies S3, S4, S5. In ARB-treated cells, the number of CCPs forming at the cell surface decreased (Fig. 4B) and the number of long-lived structures increased (Fig. 4C), indicating that ARB alters CME dynamics by slowing down CCP formation at the cell surface (Movies S6, S7, S8).

To pinpoint how ARB affects CME, we used BSC-1 cells co-expressing clathrin light chain fused to the fluorescent protein tomato (Clc-tomato) and dynamin-2 fused to GFP (Dyn-GFP). Dynamin-2 is a GTPase involved in the final step of CCV formation, recruited to membranes of fully-formed CCPs and promoting CCP pinching from the plasma membrane. In mock-treated cells, Dyn-GFP was recruited just prior to the disappearance of clathrin-coated structures (Fig. 4D left panels). Conversely, in ARB-treated cells, Dyn-GFP was recruited to coated structures but this was not associated with disappearance of the clathrin signal (Fig. 4D right panels). We sometimes observed multiple Dyn-GFP recruitments to the same frozen clathrin structures (not shown). ARB would therefore affect CME not by blocking dynamin-2 recruitment but by preventing dynamin-2-induced membrane scission.

In summary, our study provides for the first time molecular details of ARB's mechanism of action on viral entry, with the following conclusions: (i) ARB hinders HCV endosomal trafficking: virions get trapped in clathrin-positive structures and cannot be properly delivered to endosomal compartments, thereby preventing infection; (ii) ARB globally impedes CME and induces the intracellular accumulation of clathrin-coated structures, and acts at the most early stage of membrane scission leading to CCP formation; (iii) this could constitute a general mechanism of action, since ARB also efficiently hinders cell infection by VSV and reovirus which enter cells by CME as well.

Since ARB displays tropism for lipid bilayers, as we showed previously (Pécheur et al., 2007; Teissier et al., 2011), we propose that ARB, by inserting into cellular membranes, would impregnate these membranes thereby impeding the release of CCV from the plasma membrane. This effect might be at the protein level, preventing the recruitment/activation of proteins which co-act with dynamin-2 to release the CCV or at the lipid level preventing hemi-fusion/fusion to occur. We previously demonstrated that ARB inhibits membrane fusion of liposomes, we therefore favor this "membrane intoxication model" as it also explains the accumulation of HCV in endosomal compartments due to impaired fusion and cytosolic release. We recently proposed a similar mechanism of action for silibinin, a 1:1 mixture of flavonolignans silybin A and silybin B (Blaising et al., 2013).

ARB would therefore constitute a potent broad spectrum antiviral agent able to hinder the entry of several viruses infecting their host cells by CME.

Acknowledgments

We thank C.M. Rice for Huh7.5 cells, J. Dubuisson for HCVpp plasmids and antibodies, C. Chamot, O. Duc and C. Lionnet for training and help with cell imaging (PLATIM, ENS Lyon), J.J. Blaising (CERN, Geneva) for expertise on statistical analyses and J. Klinghauf for eGFP-clathrin plasmid. E-I.P. is supported by FINOVI foundation and ANRS. S.B. was supported by the Chica and Heinz Schaller foundation (Germany) and the European Union Seventh Framework Program (FP7-PEOPLE-2012-CIG) under the grant agreement n°334336. J.B. is the recipient of a PhD grant from Cluster Infectiologie Région Rhône Alpes.

Appendix A. Supplementary data

Supplementary data associated with this article can be found, in the online version, at http://dx.doi.org/10.1016/j.antiviral.2013.08.008.

References

Bartosch, B., Dubuisson, J., Cosset, F.L., 2003. Infectious hepatitis C virus pseudo-particles containing functional E1–E2 envelope protein complexes. J. Exp. Med. 197, 633–642.

Blaising, J., Lévy P.L., Gondeau, C., Phelip, C., Varbanov, M., Teissier, E., Ruggiero, F., Polyak, S.J., Oberlies, N.H., Ivanovic, T., Boulant, S., Pécheur, E.I., 2013. Silibinin inhibits hepatitis C virus entry into hepatocytes by hindering clathrin-dependent trafficking. Cell Microbiol. http://dx.doi.org/10.1111/cmi.12155. [Epub ahead of print].

Boriskin, Y.S., Pécheur, E.I., Polyak, S.J., 2006. Arbidol: a broad-spectrum antiviral that inhibits acute and chronic HCV infection. Virol. J. 3, 56.

Boriskin, Y.S., Leneva, I.A., Pécheur, E.I., Polyak, S.J., 2008. Arbidol: a broad-spectrum antiviral compound that blocks viral fusion. Curr. Med. Chem. 15, 997–1005.

Boulant, S., Kural, C., Zeeh, J.C., Ubelmann, F., Kirchhausen, T., 2011. Actin dynamics counteract membrane tension during clathrin-mediated endocytosis. Nat. Cell Biol. 13, 1124–1131.

Brooks, M.J., Sasadeusz, J.J., Tannock, G.A., 2004. Antiviral chemotherapeutic agents against respiratory viruses: where are we now and what's in the pipeline? Curr. Opin. Pulm. Med. 10, 197–203.

Brooks, M.J., Burtseva, E.I., Ellery, P.J., Marsh, G.A., Lew, A.M., Slepushkin, A.N., Crowe, S.M., Tannock, G.A., 2012. Antiviral activity of arbidol, a broad-spectrum drug for use against respiratory viruses, varies according to test conditions. J. Med. Virol. 84, 170–181.

Chai, H., Zhao, Y., Zhao, C., Gong, P., 2006. Synthesis and in vitro anti-hepatitis B virus activities of some ethyl 6-bromo-5-hydroxy-1H-indole-3-carboxylates. Bioorg. Med. Chem. 14, 911–917.

Cureton, D.K., Massol, R.H., Saffarian, S., Kirchhausen, T.L., Whelan, S.P., 2009. Vesicular stomatitis virus enters cells through vesicles incompletely coated with clathrin that depend upon actin for internalization. PLoS Pathog. 5, e1000394.

Delogu, I., Pastorino, B., Baronti, C., Nougairede, A., Bonnet, E., de Lamballerie, X., 2011. In vitro antiviral activity of arbidol against Chikungunya virus and characteristics of a selected resistant mutant. Antiviral Res. 90, 99–107.

Ehrlich, M., Boll, W., Van Oijen, A., Hariharan, R., Chandran, K., Nibert, M.L., Kirchhausen, T., 2004. Endocytosis by random initiation and stabilization of clathrin-coated pits. Cell 118, 591–605.

Haid, S., Pietschmann, T., Pécheur, E.I., 2009. Low pH-dependent hepatitis C virus membrane fusion depends on E2 integrity, target lipid composition, and density of virus particles. J. Biol. Chem. 284, 17657–17667.

Leneva, I.A., Russell, R.J., Boriskin, Y.S., Hay, A.J., 2009. Characteristics of arbidol-resistant mutants of influenza virus: implications for the mechanism of anti-influenza action of arbidol. Antiviral Res. 81, 132–140.

Maginnis, M.S., Mainou, B.A., Derdowski, A., Johnson, E.M., Zent, R., Dermody, T.S., 2008. NPXY motifs in the beta1 integrin cytoplasmic tail are required for functional reovirus entry. J. Virol. 82, 3181–3191.

Martinez, C.G., Guinea, R., Benavente, J., Carrasco, L., 1996. The entry of reovirus into L cells is dependent on vacuolar proton-ATPase activity. J. Virol. 70, 576–579.

Pécheur, E.I., Lavillette, D., Alcaras, F., Molle, J., Boriskin, Y.S., Roberts, M., Cosset, F.L., Polyak, S.J., 2007. Biochemical mechanism of hepatitis C virus inhibition by the broad-spectrum antiviral arbidol. Biochemistry 46, 6050–6059.

Schulz, W.L., Haj, A.K., Schiff, L.A., 2012. Reovirus uses multiple endocytic pathways for cell entry. J. Virol. 86, 12665–12675.

Teissier, E., Penin, F., Pécheur, E.I., 2010. Targeting cell entry of enveloped viruses as an antiviral strategy. Molecules 16, 221–250.

Teissier, E., Zandomeneghi, G., Loquet, A., Lavillette, D., Lavergne, J.P., Montserret, R., Cosset, F.L., Bockmann, A., Meier, B.H., Penin, F., Pécheur, E.I., 2011. Mechanism of inhibition of enveloped virus membrane fusion by the antiviral drug arbidol. PLoS One 6, e15874.

Villalain, J., 2010. Membranotropic effects of arbidol, a broad anti-viral molecule, on phospholipid model membranes. J. Phys. Chem. B 114, 8544–8554.

Wakita, T., Pietschmann, T., Kato, T., Date, T., Miyamoto, M., Zhao, Z., Murthy, K., Habermann, A., Krausslich, H.G., Mizokami, M., Bartenschlager, R., Liang, T.J., 2005. Production of infectious hepatitis C virus in tissue culture from a cloned viral genome. Nat. Med. 11, 791–796.